Mathematical Model for Pressure-Deformation Relationship of Miniaturized McKibben Actuators

Ashwin K.P[1] and Ashitava Ghosal[1]

[1]Indian Institute of Science, Bangalore
Email: {ashwinkp, asitava}@iisc.ac.in

Abstract

A McKibben actuator/ Pneumatic artificial muscle(PAM) is a soft actuator which has great potential in the field of bio-inspired robotics. Miniaturized versions of PAMs or MPAMs of less than 1.5 mm diameter are ideal actuators for developing surgical devices due to their compliance and high power to weight ratio. Accurate mathematical models to represent the mechanics of PAM is an ongoing research. This paper develops a mathematical model which relates the input pressure to end-point deformation of a fabricated MPAM without external loading. The developed theoretical model is validated against experimental data for MPAM of lengths 60 mm and 70 mm. The model predicts the deformation of MPAM with standard error of less than 10%. The model is also able to predict the locking angle of 54.7° at higher pressures which is a distinct characteristic of McKibben actuators.

Keywords: Miniaturized McKibben actuators, Pneumatic muscles, Actuated endoscopic instruments

1 Introduction

McKibben actuators or Pneumatic Artificial Muscles (PAM) are linear actuators which are gaining popularity in the field of flexible robotics. The device consists of a flexible inner tube(usually made of silicone) which is braided on the outside using sets of inextensible fibers woven in the form of a helix [1]. One end of the tube is sealed while compressed air is input to the tube through the other end. When the tube is pressurized, the entire device contracts or expands along the axis of tube depending on the geometric and material properties of the helix. Miniaturized versions of PAM (MPAM) of diameter less than 1.5 mm as shown in references [2] and [3] can be used for developing surgical devices since they offer high power to weight ratio and compliance in its actuated state. In an earlier work [4], a flexible end-effector using three MPAMs that can deflect an endoscopic catheter tip up to 15 mm within an approximately hemispherical surface is presented. The design is similar to a tendon driven continuum robot [5] where tendons are replaced by MPAMs to provide flexibility (see the CAD model shown in Fig. 1). Fig. 2 shows the in-house fabricated MPAM used to develop the end-effector. In order to study the kinematics of the end-effector developed using MPAMs and to apply model

based control strategies, understanding the relationship between applied pressure and deformation of MPAM is essential and this is the focus of this work.

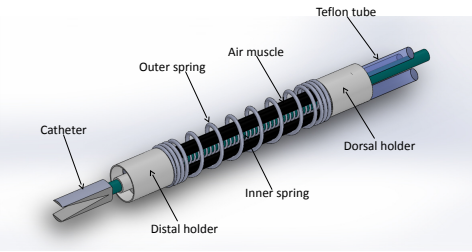

Figure 1: End-effector

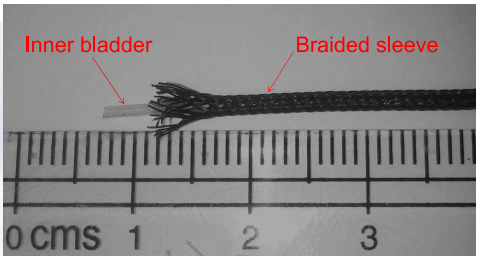

Figure 2: MPAM

Development of accurate models to predict this relationship based on the geometric and material parameters of PAM is an active topic of research. The first model to describe the statics of PAM, developed by Schulte [6], equated the input work done by applied pressure to the work done by an end-force to displace the actuator tip through a particular distance. A review paper by Tondu [7] lists the major improvements made by researchers on this basic model in subsequent years. However, with the inclusion of details such as nonlinear material modeling, friction modeling as well as the variation of MPAM profile at the ends, these models become complex, computationally expensive to simulate or vary considerably when applied on miniaturized PAMs. Hence, most of these models are not suitable for real-time control of the developed end-effector.

In this paper, a new model describing the pressure-deformation relationship of MPAM is developed. Section 2 details the proposed mathematical model starting from the equilibrium equations of a thick cylinder under inflation. In section 3, the theoretical model is compared against experimental results for validation. It is also shown that the model is able to predict the locking angle of 54.7°. Conclusions are presented in section 4.

2 Mathematical Model of MPAM

In this section, we present the developed mathematical model of an MPAM. We start by mentioning the two main assumptions on use of linear elasticity and ignoring the hysteresis present in a PAM. In reference [8], the authors describe two derivations using energy method as well as force balance method to model the statics of PAM. It is shown that the force balance method which considers the bladder as linear elastic material gives better accuracy and is simpler to implement compared to energy method which considers the inner bladder as a non-linear Mooney-Rivlin material. Hence, in the derivations presented in this work, we assume linear elastic thick cylinder model for the silicone bladder in MPAM. It may also be noted that as in the case of PAMs in general, the developed MPAM also shows hysteresis. In reference [7], it is shown that the major reason for hysteresis in a PAM are the static friction between braid strands as well as the friction between the braid strands and the bladder. Though hysteresis effects are prominent in PAMs, in the case of MPAM used in this work, the hysteresis width between the inflation and deflation phase is of same order of magnitude as the measurement

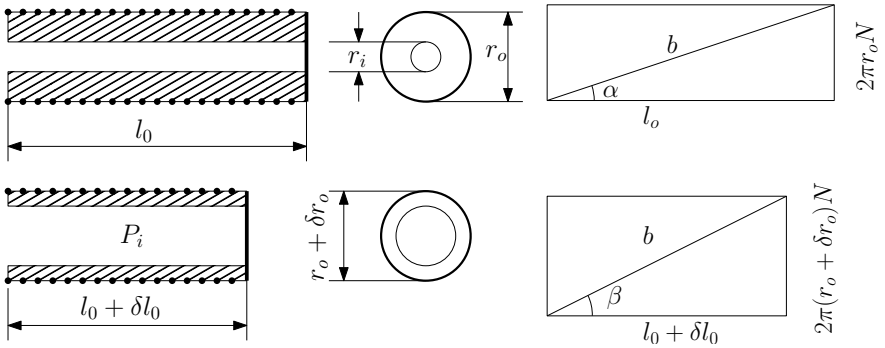

Figure 3: MPAM nomenclature

Figure 4: Braid kinematics

error band (shown in later plots). Also, since accurate friction modeling of PAM is particularly hard [7], we neglect the same in subsequent formulation.

Fig. 3 and Fig. 4 show the schematic of MPAM as well as the nomenclature which will be followed in this paper. The silicone tube has initial length l_0, outer radius r_o and inner radius r_i. The symbols δl_0 and δr_o denote the changes in length and outer radius, respectively, after applying the input pressure P_i . The initial angle of winding of MPAM, α, changes to β upon pressurization, b represents the length of a single strand of braid and N represents the number of turns in the helix.

The inflation problem of the silicone tube is solved using linear elastic equilibrium equations for thick cylinder [9] which are given as

$$\begin{aligned} \frac{\partial}{\partial r}\left[\frac{1}{r}\frac{\partial}{\partial r}\left(ru_r\right)\right] + \left(\frac{\mu}{\lambda+2\mu}\right)\frac{\partial^2 u_r}{\partial z^2} + \left(\frac{\lambda+\mu}{\lambda+2\mu}\right)\frac{\partial^2 u_z}{\partial r \partial z} = 0 \\ \frac{\partial^2 u_z}{\partial z^2} + \left(\frac{\mu}{\lambda+2\mu}\right)\left[\frac{1}{r}\frac{\partial}{\partial r}\left(r\frac{\partial u_z}{\partial r}\right)\right] + \left(\frac{\lambda+\mu}{\lambda+2\mu}\right)\left[\frac{\partial}{\partial z}\left[\frac{1}{r}\frac{\partial}{\partial r}\left(ru_r\right)\right]\right] = 0 \end{aligned} \quad (1)$$

where λ, μ are Lame's parameters, and the radial and axial displacements u_r, u_z are assumed to be functions of both r and z. The displacement in tangential direction is assumed to be zero. The boundary conditions on the radial and axial stresses, τ_{rr} and τ_{zz}, as well as the displacements on boundaries are given as

$$\tau_{rr}|_{r=r_i} = -P_i, \qquad \tau_{rr}|_{r=r_o} = -P_o, \qquad \tau_{zz}|_{z=l_0} = P_s \quad (2)$$

$$u_z(r,0) = 0, \qquad u_r(r,0) = u_r(r,l_0) = 0 \quad (3)$$

where P_o, P_s are the radial pressure on the outer surface and pressure on the axial end, respectively. The above differential equations and boundary conditions do not have analytical solutions and can only be solved using numerical techniques. However, since the length of tube is much larger compared to the radial dimensions (length to radius ratio is > 70), the variation in curvature is apparent only at far ends of MPAM. Ignoring the curvature effects[1] and assuming that u_r and u_z are

[1]The curvature effect at the end of the silicone tube is considered separately and discussed later.

only functions of r and z, respectively, Eq. (1) can be simplified to

$$\frac{\partial}{\partial r}\left(\frac{1}{r}\frac{\partial(ru_r)}{\partial r}\right) = 0$$
$$\frac{\partial^2 u_z}{\partial z^2} = 0 \tag{4}$$

Equation (4) refer to a standard problem of thick cylinder subjected to internal pressure and can be analytically solved to obtain the displacements as

$$u_r = c_1 r + \frac{c_2}{r}, \quad u_z = c_3 z + c_4$$

where $c_i,\ i = 1, 2, 3, 4$ are constants whose values can be calculated using the boundary conditions given by Eq. (2) and Eq. (3). We next consider the effect of the nylon braids and include the effect of braid with the thick cylinder model.

The expression relating axial tension on the actuator and applied pressure required to maintain equilibrium of the actuator can be found in [10]

$$P_i = \frac{F}{\pi r_o^2}\frac{\sin^2\alpha}{(3\cos^2\beta - 1)} \tag{5}$$

where F is the axial end-load. In the case of free contraction of MPAM, the term $\dfrac{F}{\pi r_o^2}$ is essentially the pressure applied on the side wall of silicone tube, P_a^b. Rearranging the above equation, we can write

$$P_a^b = P_i\frac{\left(3\cos^2\beta - 1\right)}{\sin^2\alpha} \tag{6}$$

The total pressure acting on the axial end of silicone tube can be written as

$$P_s = P_a^b + P_a^{P_i} \tag{7}$$

where $P_a^{P_i} = P_i\dfrac{r_o^2}{r_o^2 - r_i^2}$ is the component due to internal pressure.

A common modeling strategy for braid kinematics is to consider the helix as an array of pantographs [11]. From the pantograph model, the kinematics of single strand of braid can be described by

$$l_0 = b\cos\alpha, \quad l_0 + \delta l_0 = b\cos\beta \tag{8}$$
$$2\pi r_o N = b\sin\alpha, \quad 2\pi(r_o + \delta r_0)N = b\sin\beta \tag{9}$$

The above expressions assume that the MPAM remains cylindrical even after pressurizing. However, once pressurized, the ends of the MPAM will not be perfectly cylindrical since the diameter of middle section of MPAM and the diameter of ends will be different. In reference [3], this curvature effect at ends is accounted for by modifying the second expression of Eq. (8) as

$$l_0 + \delta l_0 = b\cos\beta k_1 + k_2 \tag{10}$$

where k_1 and k_2 are constants which are experimentally determined. From Eqns. (8), (9) and (10), we get

$$\delta r_0 = r_o\left(\frac{\sin\beta}{\sin\alpha} - 1\right), \quad \delta l_0 = l_0\left(k_1\frac{\cos\beta}{\cos\alpha} - 1\right) + k_2 \tag{11}$$

Since the braid and sleeve are in contact during contraction of MPAM, we can write the constraint equations $u_r|_{r_o} = \delta r_o$ and $u_z|_{l_0} = \delta l_0$. Then

$$c_1 r_o + \frac{c_2}{r_o} = r_o \left(\frac{\sin\beta}{\sin\alpha} - 1 \right) \tag{12}$$

$$c_3 l_0 + c_4 = l_0 \left(k_1 \frac{\cos\beta}{\cos\alpha} - 1 \right) + k_2 \tag{13}$$

Eq. (12) and Eq. (13) give two equations in two unknowns β and P_o which are solved numerically. Then using the second expression of Eq. (11), we can find the displacement at the free end of MPAM.

It may be noted that contraction of MPAM does not start until a particular value of pressure. This is due to a small gap between the braided sleeve and silicone tube resulting from fabrication. Hence, at the initial stage of pressurization, the silicone tube expands till a contact between tube and sleeve is established. In this stage, the pressure on the side wall, P_s, in only $P_a^{P_i}$ and the pressure on the radial surface P_o is zero. Hence, only the Eq. (13) is to be solved to obtain the value of deformed angle β and subsequently, the end-point displacement.

3 Model validation

In order to validate the proposed mathematical model for MPAM, results from theoretical model is compared with experimental data. Fig. 5 shows the experimental set-up which is used to validate the model characteristics. The set-up consists of an air reservoir of 1 liter capacity which supplies compressed air to the MPAM at a maximum of 1.03 Mpa (150 psi) pressure. The MPAM is connected to two pressure lines, one for pressurizing and the other for bleeding the air from MPAM; each controlled by individual proportional solenoid valves. An ATmel ATMEGA2560 controller board reads the pressure inside MPAM using a Honeywell pressure transducer and controls the opening or closing of the solenoid valves. The controller board is interfaced with MATLAB so that user can specify the required pressure inside the MPAM. Another controller circuit is used to sense the pressure inside reservoir and run the compressor to maintain compressed air inside reservoir at 1 MPa at all times. A high resolution camera is used to take images of contracted MPAM and the changes in length is measured using image processing. The maximum error due to measurement is approximately 0.1 mm. The experimental plots show error bars obtained from at least 5 sets of experiments. In these plots, hysteresis is not shown, and the mean value between inflation and deflation is used.

Variation of displacement according to applied pressure is determined experimentally for a MPAM of length 60 mm and is compared with the numerical simulation results obtained by solving Eq. (12) and (13) using MATLAB. The parameters used are $E = 0.9$ MPa, $\nu = 0.4999$, $\delta = 0.015$ mm, $\alpha = 36°$, $r_i = 0.25$ mm and $r_b = 0.55$ mm. The values of k_1 and k_2 for the MPAM are determined by linearly interpolating the values mentioned in reference [3] for the length of MPAM used in this study. From Fig. 6, we can see that the theoretical results match with experimental values with good accuracy (standard error of maximum 2%). Using the same parameter values, theoretical results obtained for a 70 mm MPAM in comparison with experimental values give a standard error of 8%. This

shows that the model is consistent with changes in initial length of the MPAM (refer Fig. 7). It may be noted that the error bars in the range of 100 to 400 kPa is larger than the rest of the curve due to the averaging of inflation and deflation data. The discrepancy between the theoretical and actual plots in the onset of contraction may be attributed to the fact that the developed model does not take into account the energy losses due to friction and hence predicts only the inflation characteristics.

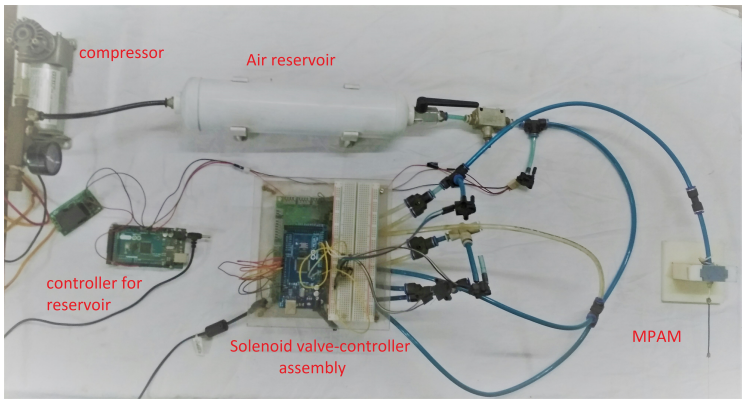

Figure 5: Experimental set-up

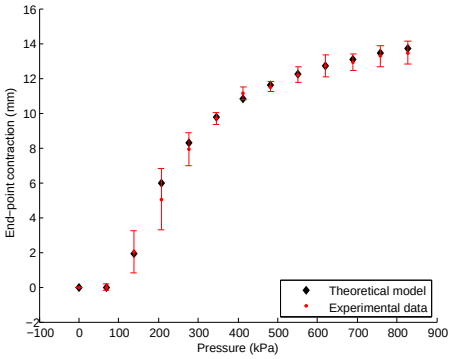

Figure 6: End-point contraction for 60 mm MPAM

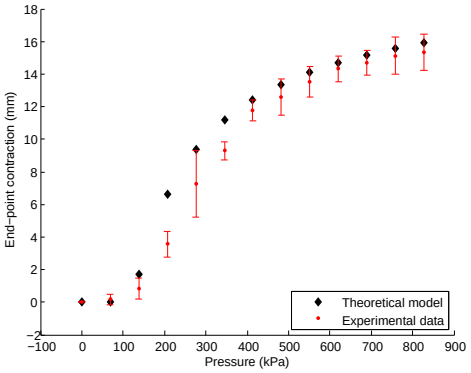

Figure 7: End-point contraction for 70 mm MPAM

From the literature, we know that the actuator contracts when the initial angle of winding is less than 54.7° while it elongates when the winding angle is more than 54.7° [10]. Additionally, as the pressure increases, the final angle of winding approaches these limiting values. The results of the theoretical model for a MPAM with a winding angle of 35°, when subjected to higher pressure, is shown in Fig. 8. It can be seen that the angle approaches 54.7° at higher pressure. It may also be noted that the pressure required to reach the locking angle with initial $\alpha > 54.7°$ is much higher than when the initial starting angle is less than 54.7° (Refer Fig. 9, $\alpha = 70°$). This result may be explained by considering the rate of change of

volume of MPAM. The volumetric strain for a volume $V = \pi r_o^2 l_0$ is

$$\frac{\delta V}{V} = 2\frac{\delta r_o}{r_o} + \frac{\delta l_0}{l_0} \tag{14}$$

For the linear elastic material used in the formulation,

$$\frac{\delta r_o}{r_o} = C_1 + \frac{C_2}{r_o^2} \text{ and } \frac{\delta l_0}{l_0} = C_3 \tag{15}$$

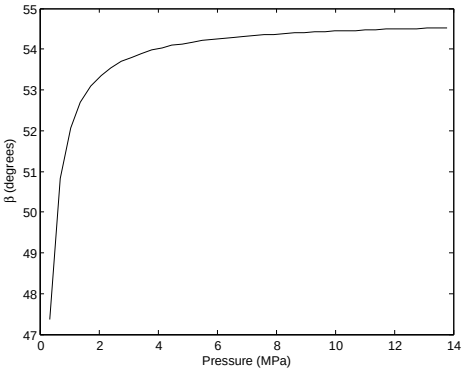

Figure 8: β vs P_i for $\alpha = 35°$

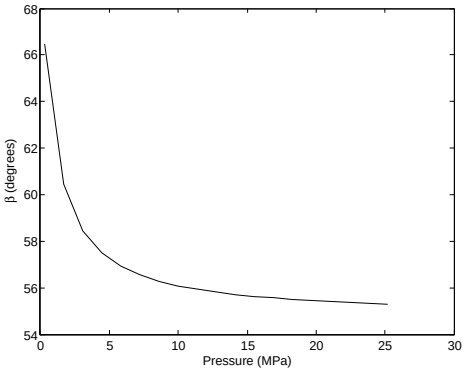

Figure 9: β vs P_i for $\alpha = 70°$

For a given pressure, the radial strain given by the first term increases by a magnitude of three orders higher than the magnitude of axial strain which is the second term. It means that the compliance of tube in radial direction is much higher compared to the axial direction. Hence, the silicone tube tends to expand radially at a faster rate when subjected to pressurization. For the case of MPAM with $\alpha > 54.7°$, the tube has to contract radially due to the kinematics of braided sleeve which is achieved only by working against the applied pressure. Hence, locking angle is reached only at larger pressures for elongation of the MPAM while it is achieved easily in the case of contraction. This observation is further verified from the experimental data mentioned in references [12] and [13] where the limiting angle is not achieved even for high pressure values.

The response to change in thickness of silicone tube is plotted in Fig. 10. We see that as the thickness increases, the initial slope of curve decreases so that the limiting value of β is reached only at high pressure. This is because the applied pressure now works against the increased elastic force due to added material. This observation is also consistent with other models available in literature.

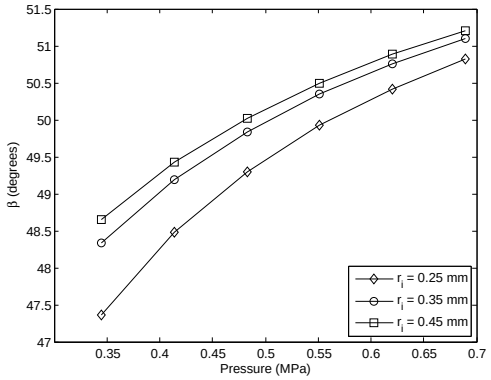

Figure 10: Variation of β w.r.t change in thickness, $r_o = 0.55$ mm

4 Conclusions

A mathematical model representing the relationship between applied pressure and deformation of Miniaturized Pneumatic Artificial Muscles is successfully developed. Unlike the existing models in literature for PAM, the developed model is considerably simple even after taking into account material properties of the tube as well as the curvature effects at the ends, making it ideal for implementing model based control strategies in real time. The numerically simulated results show very good agreement with experimental results for a 60 mm as well as 70 mm long MPAM. The model shows increase in the value of braid angle when the initial angle of winding is less than 54.7° and decrease in braid angle when the initial angle is more than 54.7°. In both cases, for higher value of applied pressure, the braid angle reaches the locking angle which further confirms the consistency of the model with the observations reported in the literature. From the developed theoretical model for the pressure-deformation relationship of MPAM, kinematics of the flexible end-effector corresponding to the values of pressure applied on MPAMs can be developed. The authors are presently working towards achieving this goal.

Acknowledgement

This work was funded in part by the Robert Bosch Center for Cyber Physical Systems (RBCCPS) at the Indian Institute of Science, Bangalore.

References

[1] R. H. Gaylord, "Fluid actuated motor system and stroking device," July 22 1958. US Patent 2,844,126.

[2] M. De Volder, A. Moers, and D. Reynaerts, "Fabrication and control of miniature mckibben actuators," *Sensors and Actuators A: Physical*, vol. 166, no. 1, pp. 111–116, 2011.

[3] S. Chakravarthy, K. Aditya, and A. Ghosal, "Experimental characterization and control of miniaturized pneumatic artificial muscle," *Journal of Medical Devices*, vol. 8, no. 4, p. 041011, 2014.

[4] K. P. Ashwin, D. P. Jose, and A. Ghosal, "Modeling and analysis of a flexible end-effector for actuating endoscopic catheters," in *Proceedings of the 14th IFToMM World Congress*, pp. 113–120, IFToMM, 2015.

[5] I. A. Gravagne and I. D. Walker, "On the kinematics of remotely-actuated continuum robots," in *Robotics and Automation, 2000. Proceedings. ICRA'00. IEEE International Conference on*, vol. 3, pp. 2544–2550, IEEE, 2000.

[6] H. Schulte, "The application of external power in prosthetics and orthotics," *The Characteristics of the McKibben Artificial Muscle, National Research Council*, vol. 874, 1961.

[7] B. Tondu, "Modelling of the mckibben artificial muscle: A review," *Journal of Intelligent Material Systems and Structures*, vol. 23, no. 3, pp. 225–253, 2012.

[8] C. S. Kothera, M. Jangid, J. Sirohi, and N. M. Wereley, "Experimental characterization and static modeling of mckibben actuators," *Journal of Mechanical Design*, vol. 131, no. 9, p. 091010, 2009.

[9] C. S. Jog, *Continuum mechanics*, vol. 1. Cambridge University Press, 2015.

[10] C.-P. Chou and B. Hannaford, "Measurement and modeling of mckibben pneumatic artificial muscles," *IEEE Transactions on robotics and automation*, vol. 12, no. 1, pp. 90–102, 1996.

[11] B. Zhou, M. Accorsi, and J. Leonard, "A new finite element for modeling pneumatic muscle actuators," *Computers & structures*, vol. 82, no. 11, pp. 845–856, 2004.

[12] D. Chen and K. Ushijima, "Prediction of the mechanical performance of mckibben artificial muscle actuator," *International Journal of Mechanical Sciences*, vol. 78, pp. 183–192, 2014.

[13] G. Krishnan, J. Bishop-Moser, C. Kim, and S. Kota, "Kinematics of a generalized class of pneumatic artificial muscles," *Journal of Mechanisms and Robotics*, vol. 7, no. 4, p. 041014, 2015.